Journal of Applied Polymer Science

Studies on the thermal and mechanical behavior of PLA-PET blends

Andrew R. McLauchlin, Oana R. Ghita
Mathematics and Physical Sciences, College of Engineering, University of Exeter, Exeter, EX4 4QF, UK
Correspondence to: A. R. McLauchlin (E-mail: a.mclauchlin@exeter.ac.uk)

ABSTRACT: The increasing use of bio-sourced and biodegradable polymers such as poly(lactic acid) (PLA) in bottle packaging presents an increasing challenge to the polyethylene terephthalate (PET) recycling process. Despite advanced separation technologies to remove PLA from PET recyclate, PLA may still be found in rPET process streams. This study explores the effects of PLA on the mechanical properties and crystallization behavior of blends of PET containing 0.5–20% PLA produced by injection molding. SEM indicates an immiscible blend of the two polymers and TGA confirms the independent behavior of the two polymers under thermal degradation conditions. Temperature-modulated DSC studies indicate that adding PLA to PET increases the rigid amorphous fraction of the PET moiety. Critical amounts of PLA induce stress oscillation behavior during mechanical testing. The mechanical behavior of the samples is explained by antagonistic interaction between increased rigid amorphous fraction and decreased fracture strength arising from an increased population of PLA microparticles. © 2016 Wiley Periodicals, Inc. J. Appl. Polym. Sci. **2016**, *133*, 44147.

KEYWORDS: amorphous; biopolymers and renewable polymers; differential scanning calorimetry; mechanical properties; properties and characterization

Received 17 February 2016; accepted 30 June 2016
DOI: 10.1002/app.44147

INTRODUCTION

Polyethylene terephthalate (PET) has become one of the most recycled plastics in Europe: in 2013, 65 billion PET bottles were recycled in Europe. Among the challenges to the quality of rPET are biodegradable polymers, one such being poly(lactic acid) (PLA), which is a biodegradable polymer of L-lactose derived by hydrolysis of plant starch.[1] The similar optical properties and density of PET and PLA preclude hand sorting and flotation separation methods, although near-infrared sorting technology is employed to separate the two materials.[2,3]

Apart from packaging, recycled PET is also used for fiber applications such as textiles although some rPET, which does not meet criteria of clarity and color for food use can be used to make straps: in 2009 about 7% of PET recyclate was used for strapping.[4–6] Although the optical properties of PET for strapping are less of a concern, the mechanical properties remain highly important, since strapping, which is likely to fail under load would present an obvious hazard. Previous studies have explored the rheological properties of PET/PLA blends as these are relevant to the blow molding process where melt flow properties must be considered. For example, in one study, it was shown that the addition of 1% or 2% dry PLA to PET had a very small effect on the melt viscosity of PET, but that the effect was much more significant if the PLA was undried, since the water present in the PLA is likely to cause hydrolysis of the PET.[4,7] Moisture has relatively little effect on the mechanical properties of modulus and tensile strength, but significantly reduces impact strength and elongation to break.[8] Where bale strapping is concerned, solid state properties such as tensile strength and elongation to break are important, but these are not measured by techniques such as melt rheology, mechanical testing can provide the necessary information about polymer behavior.

Although the processing temperature of PET (ca. 260 °C) is much higher than the typical melting temperature of PLA (ca. 180 °C), it has been shown that PLA heated under nitrogen did not appreciably begin to decompose, as indicated by the emission of gaseous breakdown products, until a temperature of 300 °C was reached.[9] However the number-averaged molecular weight (Mn) of PLA processed for 10 min in the intensive mixing conditions of a Braebender Plastograph mixer in the temperature range 150–200 °C was significantly reduced.[10] On the basis of these reports, it is therefore reasonable to assume that PLA, which has been coprocessed with PET is unlikely to have undergone decomposition other than chain scission during the short residence time in an injection molder barrel.

Given the current efficiency of optical sorting systems for rigid plastics it might be expected that the amounts of PLA passing

Additional Supporting Information may be found in the online version of this article.

Table I. Calculated Hansen Solubility Parameters for PLA and PET[20]

Polymer	Molar volume (V) (cm^3 mol^{-1})	Dispersive component δ_D	Polar component δ_P	Hydrogen bonding component δ_H	Hansen solubility parameter δ_T
PLA	47.1	14.0	12.9	10.0	21.5
PET	144.5	16.8	10.4	11.0	22.6

through a system and appearing in the recyclate will be less than 1%, but, there are few published studies on the effect on mechanical properties of PET when melt-processed with PLA. One study reporting the inclusion of up to 5% PLA in PET by melt blending concluded that 2% PLA or less had negligible effect on tensile strength. An increase in elastic modulus by inclusion of up to 2% PLA was explained by the reinforcing effect of the PLA, which had a greater modulus (1710 MPa) than that of the PET used (1288 MPa).[7] From a small increase in the enthalpy of fusion, the authors concluded that inclusion of up to 1% PLA increased the crystallinity of the PET while greater amounts reduced it. However, the variance in the values obtained was not indicated and the small differences involved could easily be explained by experimental error. Furthermore, it has been shown that initial crystallinity cannot be inferred by simply considering the enthalpy of fusion, due to dynamic changes in the crystallinity of PET during the DSC analysis itself.[11] In another study, PLA was melt blended with PET at 20% and 40% addition, with the authors reporting a 250% increase in Young's modulus and 80% reduction in impact strength according to ASTM D1822.[12] However there is no data for PLA concentrations between 5% and 20%, so the behavior of intermediate mixtures is unknown. Furthermore, these studies are based on intensive mechanical mixing and to date, to our knowledge no-one has investigated the properties of blends arising from processes such as injection moulding, which is one aspect of this study.

PET exhibits multiple melting endotherms, which have been studied by superfast differential scanning calorimetry (DSC) and temperature modulated DSC and consequently have been shown to be due to simultaneous melting and recrystallization of the crystal lamellae of PET.[13,14] Up to three endotherms have been observed, their appearance and intensity reflecting the conditions under which crystallization has taken place. Thus the lowest temperature endotherm represents the melting of imperfect lamellae formed during secondary crystallization and consequently is not always present, while the next lowest isotherm represents the original crystalline lamellae. The highest endotherm represents melting of primary lamellae, which have been thickened by recrystallization.[14] These studies have focused on interpreting the behavior and appearance of these endotherms terms of the thermal history of the PET and in particular the crystallization conditions but the effects of inclusion of other polymers or contaminants are less well studied. Thus in one study it was found that the presence of 10% or more of PLA in the PET/PLA blend interfered with this phenomenon such that the higher melting endotherm, which is the product of the recrystallization disappeared.[15]

Semicrystalline PET comprises three phases: a solid crystalline phase; a liquid mobile amorphous phase (MAF) and a rigid amorphous phase (RAF) with only the MAF contributing to the change in heat capacity over the glass transition temperature as the RAF will not undergo relaxation at this temperature.[16,17] While PLA by comparison contains very little RAF, it has been shown that increasing amounts of PLA up to 10% can increase the RAF of PET on isothermal crystallization from the melt, although the mechanical properties of these blends were not reported.[15,18]

The miscibility of PET and PLA has been investigated by micromorphological and DSC studies. Hence examination of melt compounded PET/PLA blends by scanning electron microscopy has indicated the immiscibility of the two polymers by the existence of beads of PLA in a matrix of PET at concentrations of PLA up to 2%, while 5% PLA or more led to a clear biphasic morphology.[7] The same authors also noted poor adhesion of the PLA beads to the PET matrix, similar to that reported for mixtures of PET with other immiscible contaminants.[19] The net effect of this is that as little as 0.5% PLA leads to cloudiness in PET thereby rendering it unusable for bottles or other applications requiring optical clarity. However in another study, PET/PLA blends containing up to 90% PLA were produced by solution casting from hexafluoro-2-propanol.[15] The authors reported that PET was able to crystallize in all the blends studied but that PLA did not crystallize when present at less than 90%. Furthermore, these blends showed a single concentration-dependent glass transition, indicating miscibility.[15] The miscibility of two or more polymers can be predicted by comparing their solubility parameters, which describe the surface tension of a polymer in terms of three parameters: δD for Dispersion (van der Waals), δP for Polarity (related to dipole moment), and δH for hydrogen bonding. A further parameter which is often considered is the molar volume, which is a measure of the size of the repeating monomer unit. The Hansen solubility parameters for PET and PLA are sufficiently close as to suggest that they ought to be miscible (Table I) on thermodynamic grounds. However, the structure of PET is dominated by bulky aromatic rings, which is reflected in its higher molar volume (V) than PLA and, which may account for the separation of these polymers in both melt and solid states.

The literature to date reports either the properties of PET containing small amounts of PLA produced by melt blending or the properties of blends containing greater amounts of PLA obtained by solution casting. Beyond this, there are few, if any, reports on the effect of PLA on the physical properties of PET despite the unpopularity of PLA in the PET recycling industries. This study reports the properties of blends of PET containing 0.5% to 20% PLA produced by a melt blending technique, i.e., injection molding so as to reflect amounts of PLA, which may be encountered in a recycling situation, and discusses the effects

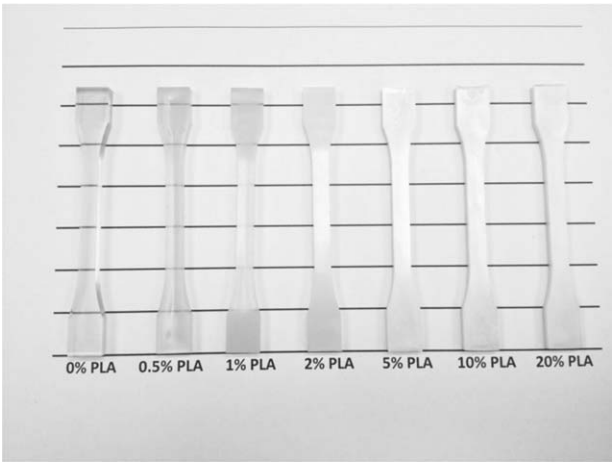

Figure 1. Injection molded test pieces of PET containing 0% to 20% PLA.

of PLA on the mechanical properties and crystallization behavior.

Whereas previous reports have studied inclusion of up to 40% PLA by melt compounding and larger amounts of PLA have only been studied by solution casting, currently data on the behavior of this binary system in the concentration range 5–20% is missing. In this article, we investigate the effect of 0.5–20% PLA on the microstructure of PET and relate this to the observed trends in key mechanical properties. DSC was used to investigate the nature of the blend of the two polymers while SEM analysis was used to investigate their miscibility. Mechanical testing focused on tensile strength and Charpy impact resistance as physical parameters relevant to the likely end-use of PET, which does not meet optical clarity standards. The mechanical behavior of the samples is explained by antagonistic interaction between increased rigid amorphous fraction and decreased fracture strength arising from an increased population of PLA microparticles. The proportion of RAF in PET increased with increasing PLA, increasing the likelihood of stress oscillation behavior under dynamic tensile testing until offset by the weakening effect of PLA microparticles in the polymer blend.

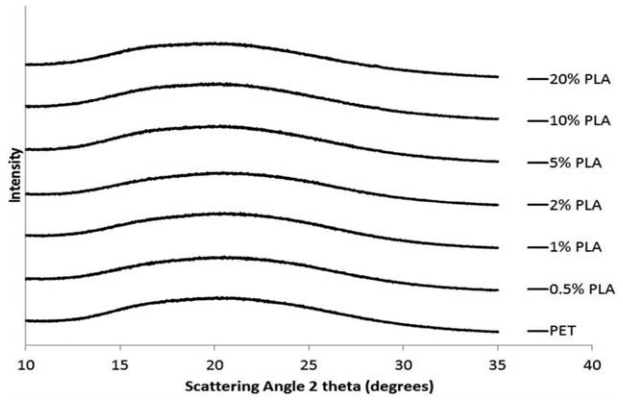

Figure 2. X-ray diffractograms of injection molded PET and PET/PLA blends.

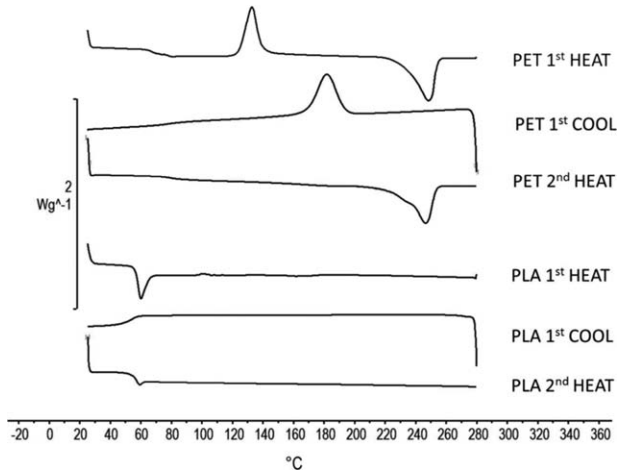

Figure 3. Thermograms of injection molded virgin PET and virgin PLA pellet used in the study.

MATERIALS

Hisun Revode 201 injection molding grade PLA of weight-average molecular weight (M_w) = 150,000 Daltons containing 3.5% D-lactate was obtained from Bioresins.eu (Olney, Bucks MK46 5FP UK). Melinar Laser+ injection grade PET (intrinsic viscosity: 0.82 dl/g) was obtained from Distrupol Limited, UK. PET resin was dried at 107 °C for 8 h and PLA was dried at 40 °C prior to processing trials.

METHODS

Injection Molding

Injection molding was done with a Battenfeld HM40 4/130 Injection Moulder. The nozzle and barrel temperatures were 265 and 260 °C, respectively and the injection and holding pressures were 480 and 300 bar, respectively. The tool produced one tensile "dog bone" and one impact bar per shot. The holding time was 4 s with a tool temperature of 25 °C. Full injection molding conditions have been described previously.[21] Blends of PET containing 0.5%, 1%, 2%, 5%, 10%, and 20% w/w PLA were prepared by preblending the dried resin pellets in a container before adding to the feed hopper of the injection molder. The concentration of the PLA in PET was calculated from the weights of the components in each mixture.

X-ray Diffraction Analysis

X-ray diffraction analysis (XRD) was performed on the injection moulded parts directly using a Bruker D8 Advance X-ray diffractometer with a LynxEye detector, operating at 40 kV voltage and 40 mA current using CuK_α radiation ($\lambda = 0.1542$ nm) in the range 10°–30° 2 theta (2θ) in 0.03° increments. The specimens had no additional treatment prior to analysis.

Mechanical Testing

Tensile testing was done according to ASTM-D638 using a Lloyd instruments EZ20 extensometer with 20 kN load cell and an extension rate of 50 mm/min. Ten specimens per treatment were tested. Impact testing (ten specimens per treatment) was done according to ISO 179-1 on unnotched bars (10 × 4 × 80 mm^3) using a Resil Impactor Junior (CEAST Instruments). All testing was carried out at ambient temperature (20 °C).

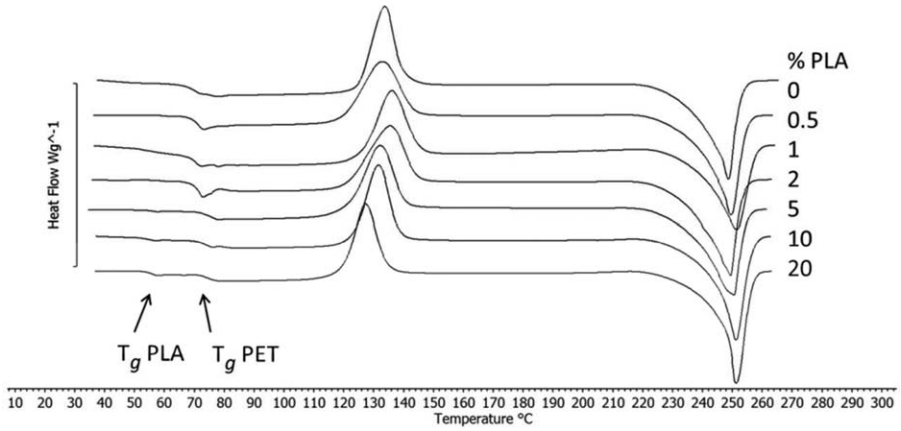

Figure 4. Thermograms (first heat) of injection molded PET/PLA blends, showing cold crystallization and fusion. Glass transitions of PLA and PET are indicated by arrows. Curves are displaced vertically for clarity.

Differential Scanning Calorimetric Analysis

Specimens (10 mg) were analysed on a Mettler Toledo D820 differential scanning calorimeter. The specimen was heated to 280 °C at 10 °C/min to remove thermal history, cooled to 25 °C at the same rate and finally heated again to 280 °C at the same rate. Enthalpies of cold crystallization, melting (fusion) and recrystallization on cooling were derived from the area of the peak in each case and normalized to the sample weight. The derived enthalpy was corrected for the PLA content using eq. (1).

$$\Delta H\text{corr} = \Delta H/[(1-x)] \quad (1)$$

where:

ΔHcorr, the corrected enthalpy (J g^{-1}); ΔH, the normalized enthalpy of the transition (J g^{-1}); x, the fraction of PLA in the blend.

When amorphous material is heated through its glass transition temperature, the heat capacity increases stepwise and the height of the step is proportional to the amount of mobile amorphous phase in the material: a purely crystalline material does not show a glass transition. The increase in heat capacity is therefore a measure of the proportion of mobile amorphous phase. The change in heat capacity (ΔCp) over the glass transition was measured using temperature-modulated DSC since this technique is more sensitive to small changes in this parameter.[21] Specimens were heated at 3 °C × min^{-1} from 30 to 90 °C, which covered the glass transition of PET with a temperature amplitude of 1 K and a period of 30 s.

The proportion of mobile amorphous fraction (φ_{MA}) in the blends was calculated by a method validated for PET-PLA mixtures according to eq. (2).[15]

$$\varnothing_{MA} = \frac{\Delta C_p^{Meas}(T_g)}{\left[\left(\Delta C_p^{PET}(T_g)\,W^{PET}\right)+\left(\Delta C_p^{PLA}(T_g)\,W^{PLA}\right)\right]} \quad (2)$$

where $\Delta C_p^{Meas}(T_g)$ is the increment in heat capacity measured over the T_g of PET; ΔC_p^{PET} is the increment for 100%

Table II. Thermal Properties (First Heat) of Injection-Molded PET Blends Containing 0.5–20% PLA

	First heat						
% PLA	T_g 1H (°C)	T_{cc} 1H (°C)	ΔH_{cc} 1H J g^{-1}	ΔH_{cc} $1H_{corr}$. J g^{-1}	T_m 1H (°C)	ΔH_m 1H J g^{-1}	ΔH_m $1H_{corr}$ J g^{-1}
0	69.5 ± 0.5	133.0 ± 0.5	26.5 ± 0.9	26.5 ± 0.9	248.1 ±0.6	−37.3 ± 0.7	−37.3 ± 0.7
0.5	70.7 ± 0.3	136.5 ± 0.3	26.5 ± 0.5	26.6 ± 0.5	250.2 ±1.3	−37.2 ± 0.4	−37.4 ± 0.4
1	69.6 ± 0.6	131.2 ± 1.1	26.4 ± 0.9	26.7 ± 0.9	249.6 ±0.3	−39.2 ± 0.7	−39.6 ± 0.8
2	70.4 ± 0.3	135.0 ± 0.2	26.9 ± 0.6	27.4 ± 0.6	248.9 ± ±0.3	−38.1 ± 0.8	38.9 ± 0.8
5	74.0 ± 0.6	131.0 ± 1.3	24.0 ± 1.4	25.3 ± 1.5	249.5 ± 0.8	−39.2 ± 3.1	−41.3 ± 3.3
10	72.0 ± 0.6	131.4 ± 0.3	22.7 ± 4.4	25.2 ± 4.9	251.8 ± 0.7	−40.3 ± 0.1	−44.8 ± 0.1
20	72.4 ± 2.5	126.9 ± 2.9	22.0 ± 1.7	27.5 ± 0.6	250.6 ± 0.4	−38.9 ± 0.9	−48.7 ± 0.4

T_g, glass transition temperature; T_{cc}, temperature of cold crystallization.
ΔH_{cc} 1H, measured enthalpy of cold crystallisation, first heat.
ΔH_{cc} 1H corr., Normalized enthalpy of cold crystallization, first heat, corrected for PLA content.
T_m, melting temperature, first heat.
ΔH_m 1H, measured enthalpy of melting, first heat.
ΔH_m 1H corr, Normalized enthalpy of melting, first heat, corrected for PLA content.

Table III. Thermal Properties (First Cool and Second Heat) of Injection-Molded PET Blends Containing 0.5–20% PLA

	First cool			Second heat			
% PLA	T_c 1C °C	ΔH_c 1C J g^{-1}	ΔH_c 1C corr. J g^{-1}	T_g 2H °C	T_m 2H °C	ΔH_m 2H J g^{-1}	ΔH_m 2H corr. J g^{-1}
0	182.1 ± 0.2	35.2 ± 1.2	35.2 ± 1.2	79.0 ± 0.8	246.4 ± 0.2	−36.7 ± 0.1	−36.7 ± 0.1
0.5	193.2 ± 1.2	37.9 ± 0.7	38.0 ± 0.7	79.4 ± 0.5	246.8 ± 0.1	−35.2 ± 0.8	−35.4 ± 0.8
1	196.5 ± 0.5	39.5 ± 0.5	39.9 ± 0.5	78.7 ± 0.4	247.1 ± 0.0	−35.8 ± 0.2	−36.2 ± 0.2
2	195.0 ± 0.3	38.5 ± 0.9	39.3 ± 0.9	78.3 ± 0.3	246.8 ± 0.2	−35.8 ± 0.3	−36.5 ± 0.3
5	200.0 ± 1.8	36.9 ± 1.0	38.8 ± 1.1	76.8 ± 5.3	248.1 ± 0.9	−33.9 ± 0.9	−35.6 ± 0.9
10	202.4 ± 0.5	38.4 ± 0.9	42.7 ± 1.0	77.6 ± 1.2	248.8 ± 0.7	−31.1 ± 5.8	−38.1 ± 2.2
20	204.0 ± 1.0	35.9 ± 1.4	44.9 ± 1.7	76.9 ± 0.2	248.0 ± 0.4	−32.6 ± 0.8	−40.7 ± 1.0

T_c 1C, crystallization temperature, first cool.; ΔH_c 1C, measured enthalpy of crystallization, first cool; ΔH_c 1C corr., normalized enthalpy of crystallization, first cool, corrected for PLA content; T_g 2H, glass transition temperature, second heat; T_m 2H, melting temperature, second heat; ΔH_m 2H, measured enthalpy of melting, second heat; ΔH_m 2H corr., normalized enthalpy of melting, second heat, corrected for PLA content.

amorphous PET (obtained from the ATHAS data bank); ΔC_p^{PLA} is the measured increase in heat capacity for PLA over the T_g of PET.

Thermal Gravimetric Analysis (TGA)

Thermogravimetric analysis (TGA) was performed on one specimen per treatment using a Mettler-Toledo TGA/DSC1 Thermogravimetric Analyzer. The specimen (10 mg) was heated in an alumina crucible from 50 to 650 °C at 10 °C min^{-1} under nitrogen gas.

SEM Investigation

To study the micromorphology of the PET/PLA blends, the samples were cooled in liquid nitrogen and then broken to give brittle failure surfaces. To check for artefacts created by freezing, samples were also fractured without freezing. All specimens were cut, mounted on aluminum SEM stubs using conductive adhesive pads and coated with palladium/gold. Scanning electron microscopy was carried out on a HITACHI S3200N scanning electron microscope.

RESULTS AND DISCUSSION

Examples of the test specimens produced by injection moulding are shown in Figure 1. The haziness of the pieces increased with increasing PLA content such that PET containing 5% PLA or more were effectively opaque. Even small amounts of PLA (<0.1%) will produce detectable haze in PET and this is the principle reason for its rejection by PET recyclers.[23] X-ray diffraction analysis (Figure 2) revealed that all the injection-moulded samples were amorphous, since there were no peaks corresponding to crystalline forms of either PET or PLA, both of which would have been seen in the range 10°–30° 2 theta.[15]

Differential Scanning Calorimetric Analysis

The DSC thermograms of injection molded PET and virgin PLA are shown in Figure 3. The PLA exhibited a clear glass transition but neither cold crystallization, melting nor crystallization on cooling from the melt, which indicated that this PLA was amorphous, therefore all crystallinity observed in the DSC studies was due to PET alone. The PET exhibited a glass transition and cold crystallization during the first heat, showing that there was both amorphous and crystallizable PET present and therefore that the polymer was quenched in the injection molding process. Thermograms of the first heat of all the samples showed a clear glass transition for PET around 70 °C, while a glass transition around 55 °C, which was taken to be due to PLA, was apparent in the blends containing 5% or more PLA (Figure 4). There was no evidence of a glass transition between these temperatures, which confirms that the blend was

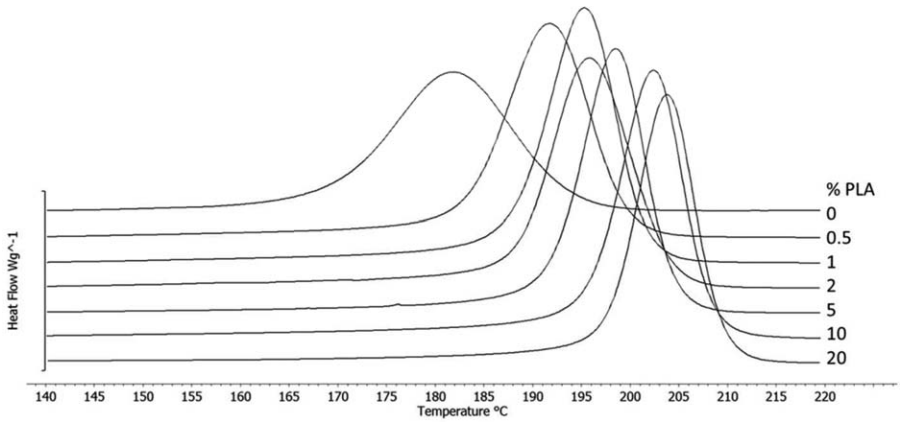

Figure 5. Thermograms (first cool) of injection molded PET/PLA blends containing 0–20% PLA, showing recrystallization exotherms. Curves are displaced vertically for clarity.

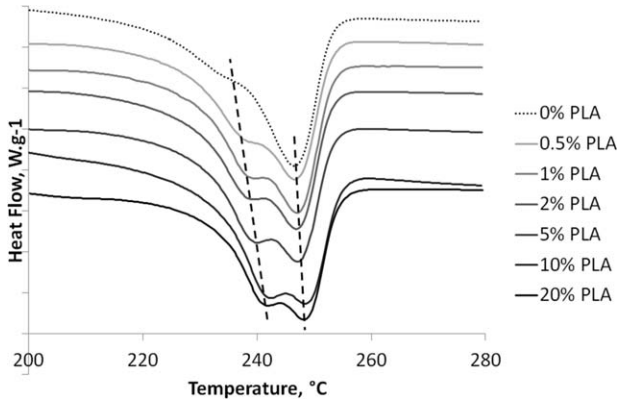

Figure 6. Thermograms (second heat) of injection molded PET/PLA blends containing 0–20% PLA, showing melting endotherms. Curves are displaced vertically for clarity.

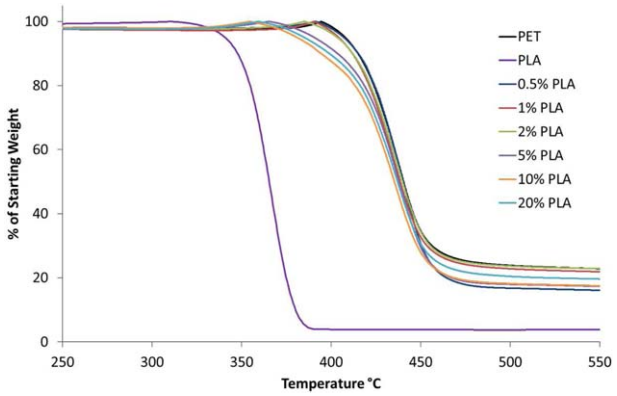

Figure 7. Percentage weight loss of PET/PLA blends as a function of temperature. [Color figure can be viewed in the online issue, which is available at wileyonlinelibrary.com.]

immiscible. Stress relaxation over the T_g of PET was seen in the samples containing 0–2% PLA, but not in those containing larger amounts. This can interfere with measurement of the change of heat capacity over this transition when conventional DSC is used, but in this case by using mDSC, the stress relaxation did not appear in the heat capacity trace and so a reliable value for *delta* Cp can be obtained.

Table II summarizes the thermal properties of the injection molded PET/PLA blends produced for this study. During the first heating phase, all samples showed a glass transition for PET, but the glass transition for PLA was only discernible in when PLA was present at 10% or greater. The first heat glass transition temperature and first heat melting temperature of PET were not significantly affected by the presence of PLA, which is consistent with other findings.[7]

All samples exhibited cold crystallization during the first heat, because the rapid cooling during the injection molding process prevented complete crystallization of the PET, consequently this crystallization process resumed on heating during the DSC analysis. The measured enthalpy of cold crystallization (shown as "ΔH_{cc} 1H" in Table II) of the whole sample, as derived from the thermograms, apparently decreased with increasing PLA content. However, the PLA content of the sample has to be considered, since the PLA itself does not crystallize as was demonstrated by running a sample of PLA alone (Figure 3), therefore a correction must be applied and this equation is given in the description of the method. When this correction (shown as "ΔH_{cc} $1H_{corr}$" in Table II) was applied, it can be seen that there was no significant change in the normalized cold crystallization enthalpy of the PET, indicating that PLA had no effect on PET crystallization during cooling in the mold and therefore the amount of crystallizable PET was independent of the PLA added. A similar correction was applied to the enthalpies of fusion and this revealed that the normalized enthalpy of fusion of the PET increased with increasing PLA, this effect being most evident in the 5%, 10%, and 20% treatments. The fact that the cold crystallization enthalpy remained constant while the melting enthalpy increased might invite the conclusion that initial crystallinity increased with increasing PLA content. However, the X-ray diffractograms show clearly that all the injection-molded samples of PET/PLA blend were in fact amorphous. The increase in melting enthalpy can therefore be explained by an increase in the amount of crystallinity developed in the specimen as it was heated during the DSC analysis, brought about by nucleation either from the added PLA or shorter chains resulting from polymer chain scission on heating.[10] It has been shown that PET, when heated, undergoes melting and recrystallization between the glass transition temperature and the final melting, processes which are revealed by modulated DSC but not by conventional DSC.[14] Consequently, any difference between the enthalpies of cold crystallization and fusion of a sample of PET does not necessarily indicate the presence of initial crystallinity, as confirmed in this study by the XRD analysis. However, an additive which promotes the recrystallization during the heating phase of the DSC analysis, will increase the melting enthalpy.

Table IV. Mobile and Rigid Amorphous Fraction of PET/PLA Blends Obtained by Injection Molding

%PLA in PET/PLA blend	Mobile amorphous fraction (φ_{MA})	Rigid amorphous fraction (φ_{RA})
0	0.80 ± 0.06	0.20
0.5	0.69 ± 0.07	0.31
1	0.73 ± 0.04	0.27
2	0.71 ± 0.02	0.29
5	0.72 ± 0.05	0.28
10	0.70 ± 0.01	0.30
20	0.70 ± 0.01	0.30

During the first cooling phase, pure PET crystallized at 182 °C on cooling from the melt (Figure 5) but in the presence of PLA, the crystallization temperature increased with increasing PLA to 204 °C, which again suggests a nucleating effect (Table III). The glass transition temperatures of the samples, measured during the second heat, were higher than the values obtained in the first heat. This is consistent with the results of other workers who observed that the glass transition of quenched amorphous PET was lower than that of semicrystalline PET obtained by

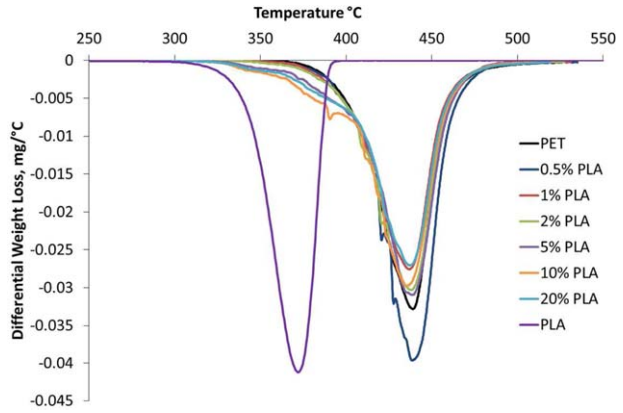

Figure 8. Differential weight loss of PET/PLA blends as a function of temperature. [Color figure can be viewed in the online issue, which is available at wileyonlinelibrary.com.]

controlled cooling.[15] However, they also found that the presence of 20% PLA lowered the T_g by ~20 °C, whereas in our study, PLA had little effect on the glass transition of the PET.

As discussed in the introduction, PET can exhibit a double melting endotherm due to melting and recrystallization and this was also seen in the samples prepared in this study (Figure 6), which showed an endotherm (I) at 238 °C, which represents the crystalline PET present in the specimen at the start of the second heating cycle, followed by a higher temperature endotherm (II) whose peak was at 246 °C. In contrast to other investigators, we found that increasing the amount of PLA in the blend increased the area of endotherm (I). If endotherm (I) is taken to represent melting of crystals formed during the first cool cycle of the analysis, then, endotherm (II) represents melting of PET crystals formed during recrystallization and again this can be explained by a nucleating effect of PLA leading to the formation of a larger population of crystallites with a lower melting temperature: the greater the amount of PLA, the greater the population of these crystallites.

The mobile amorphous fraction (φ_{MA}) of injection molded PET was 0.8 (Table IV); whereas that of the PET-PLA blends varied around 0.7, as calculated by using eq. (2) given in the Experimental Method. Since the injection-molded samples all demonstrated negligible crystallinity, as shown by XRD analysis (Figure 2), the remainder of the amorphous moiety must therefore be present as rigid amorphous fraction (RAF). The presence of amorphous phase additional to the mobile amorphous phase is supported by dynamic thermal mechanical analysis (DTMA), the results of which are presented as Supporting Information. Blending PLA into the PET therefore increased the rigid amorphous fraction at the expense of mobile amorphous fraction. Earlier in this article it was proposed that enhanced crystallization of PET from the melt in the presence of PLA may have been due to a nucleation effect of short chain degradation products of PLA: these same degradation products may facilitate the transformation of mobile amorphous to rigid amorphous fraction in the injection molding phase, although the rapid cooling arrested the full transition from RAF to crystalline phase, that has been proposed for PET.[18] This process could take place without necessarily involving transesterification reactions between PET and PLA, as has been proposed by others.[7]

Thermogravimetric Analysis

The weight loss curves over the range 205–550 °C are shown in Figure 7. PET showed the highest onset of degradation around 340 °C and while the lower amounts of PLA, i.e., 0.5%, 1%, and 2%, slightly decreased the onset of rapid degradation, inclusion of 5% or more PLA drastically reduced the onset temperature of degradation as well as the onset temperature of rapid degradation. PLA showed the lowest residual weight (5% of the starting mass) at 550 °C, due to its aliphatic nature, while PET showed a higher residual weight (22% of the starting mass). These differences can be explained partly by PLA containing a greater proportion by weight of embodied oxygen, so that more of the carbon can be lost as carbon dioxide and carbon monoxide, while PET has a lower oxygen content so that less carbon can be volatilized, added to which is the presence of aromatic rings, which tend to be resistant to thermal degradation.

The first derivative plots of the degradation region (Figure 8) provide a more sensitive indication of the onset of thermal degradation and also reveal features during the major mass loss phase of the analysis. Thus in this experiment, PLA showed a degradation onset at 296 °C, with a maximum degradation rate at 369 °C and ending at 399 °C, while PET degraded between 368 and 500 °C, with a maximum rate at 439 °C. One of the issues with PLA contamination of PET is its poor thermal stability relative to PET and this is evident in the TGA traces. The temperatures used in the injection moulding were lower than the onset temperature of PLA degradation so it is unlikely that PLA would show appreciable thermal degradation during injection molding. The first derivative plot also revealed that PLA and PET both underwent single degradation events and that adding PLA in any amount did not change the temperature of this derivative peak, indicating there was no effect on the temperature of maximum mass loss. However, the higher amounts of PLA (5%, 10%, and 20%) reduced the onset temperature to around 320 °C, which was within the degradation range for PLA. This suggests that the PLA was not stabilized by its inclusion into PET, since at the degradation onset temperature, both

Table V. Weight Loss of PET/PLA Blends over the Degradation Temperature Range of PLA (296–399°C), Corrected for PET Weight Loss over the Same Range

%PLA in PET/PLA blend	% weight loss between 296 and 399 °C	% weight loss corrected for weight loss due to PET
0	4.1	(0)
0.5	4.0	−0.1
1	5.6	1.5
2	6.0	1.9
5	9.8	5.7
10	14.1	10.1
20	19.2	15.1

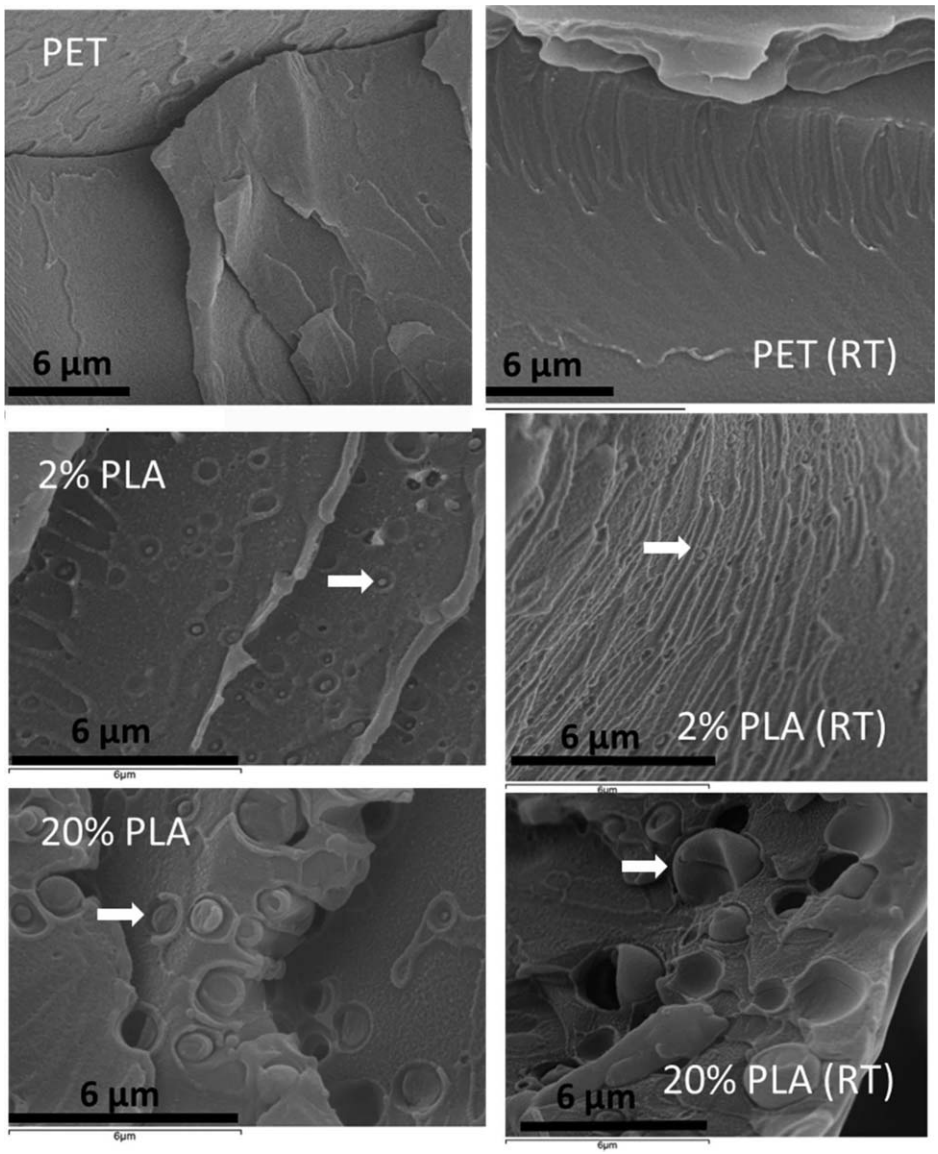

Figure 9. SEM images (6,000× magnification) of fractured injection molded PET containing zero, 2% and 20% PLA. PLA beads are indicated by white arrows. Samples labeled 'RT' were fractured at room temperature, all other samples were frozen in liquid nitrogen before fracturing. The scale bar in each image represents 6 µm.

polymers would have been completely molten and phase separation, as indicated in the electron micrographs, is likely to have occurred, leaving the PLA susceptible to degradation during the thermal analysis. There was good agreement between the percentage weight loss in the degradation range for PLA and the PLA content, after correcting for the weight loss of PET (Table V) although the weight loss of the sample containing 20% added PLA was less than expected. A number of small peaks such as those appearing around 375 °C indicate sporadic decomposition of material less stable than PET. At this temperature both polymers would have been molten, so these small peaks may represent decomposition of droplets of PLA.

Scanning Electron Microscopy

The micromorphology of the injection moulded samples containing 0%, 2%, and 20% is seen in Figure 9, which shows that the PLA was present as beads embedded in the PET matrix in the case of 2% and 20% PLA: these inclusions were absent in the PET itself and therefore were a product of the PLA since the beads increased in size with increasing PLA content and being immiscible with PET, the molten PLA assumed a spherical shape due to surface tension effects, giving rise to the spherical shape of the droplets on cooling. In the specimen containing 2% PLA the beads were clearly embedded in much larger cavities, indicative of some shrinkage of the polymers. The PLA used in this study was amorphous and therefore would not exhibit shrinkage due to crystallization although some densification due to cooling might be expected. The structure of beads within voids was seen in both nonfrozen and frozen samples and therefore not an artifact of the freezing process. In the sample containing 20% PLA, there was evidence that the beads were elongated in the direction corresponding to the direction

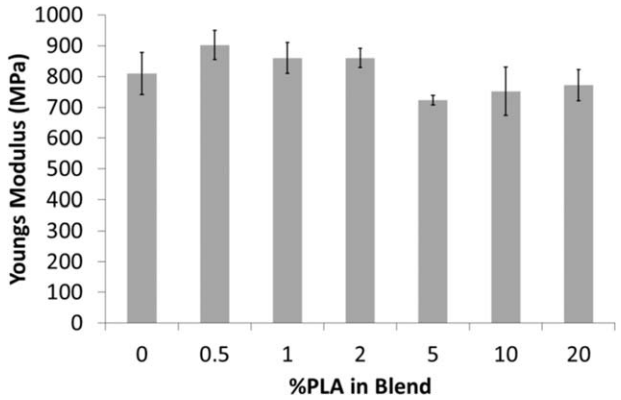

Figure 10. Young's modulus of injection-molded PET/PLA blends.

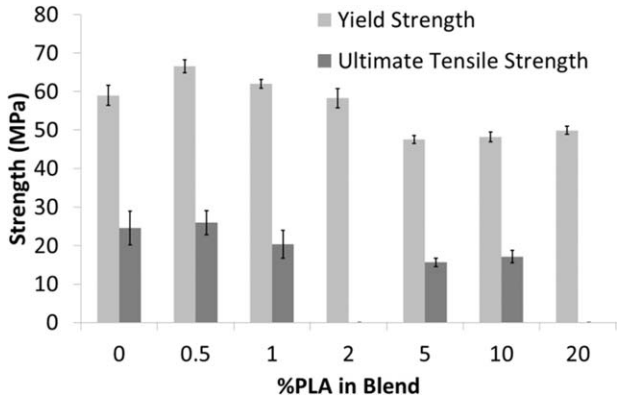

Figure 11. Yield strength and tensile strength of injection-molded PET/PLA blends.

of flow in the molded part, suggesting that the flow of polymer melt had some effect in aligning the PLA inclusions. In all the images it can be seen that the PLA and PET are not bonding in any way, despite their similar Hansen solubility parameters and therefore the PLA would contribute to the weakening of the PET as seen in the reduction in mechanical properties, discussion of which now follows.

Mechanical Properties

The tensile moduli of the specimens are shown in Figure 10. While adding up to 2% PLA raised the modulus relative to the control value, adding 5% of more of PLA reduced it by about 10%. The initial increase in modulus can be explained by the increase in the proportion of rigid amorphous fraction (RAF) detected by thermal analysis while the decrease was possibly due to the disruptive effect of the PLA microparticles in the matrix. The voids surrounding these inclusions interfere with stress transfer, thereby reducing the modulus, as noted by Leclair and Favis.[23] The PLA itself cannot play any role in the mechanical properties of these materials since there is evidently no interface with the PET as shown by SEM examination.

A similar pattern is seen in the yield strength (Figure 11), which was variably affected by up to 2% PLA, but 5% or more PLA reduced the yield strength significantly. Ultimate tensile strength (UTS) decreased with increasing PLA content up to 10% PLA; at 20% most of the specimens showed brittle failure so UTS is not shown for this PLA content. The UTS of the 2% PLA samples was anomalously high and therefore not presented in the figure, the reason for this is discussed later.

Adding as little as 0.5% PLA reduced the Charpy impact strength of PET from 114 to 98 KJ $\times$ m^{-2} and further reduction was seen when the PLA was increased to 5% or greater (Figure 12). The specimens became noticeably more brittle and inclined to shatter into smaller fragments at higher PLA contents. This brittleness can easily be explained by the increase in the population and size of PLA beads in the PET matrix. These beads interfered with the structural integrity of the matrix, and did not bond with the PET, as shown by the SEM images, which revealed voids around the PLA inclusions.

The stress–strain curves for the injection molded samples are shown in Figure 13. The elongation to break for control PET in this experiment was around 400%, but this was drastically reduced to below 60% by inclusion of 0.5% and 1% PLA, indicating that contamination with PLA at these concentrations can cause serious embrittlement of the samples. The 20% PLA samples also showed wide variation in strain to break, with the majority of the samples failing at 5% strain or less, although two samples broke at 200% elongation. Given that the DSC XRD analyses showed no effect of these amounts of PLA on initial crystallinity, the reduction in elongation to break is more likely to be due to a physical effect of the microbeads of PLA and the surrounding voids.

Interestingly, all the samples with 2% PLA that were tested showed stress oscillation behavior, with an onset at 250% strain and which resulted in overall strain hardening and consequently anomalously high UTS of 34.1 MPa, with elongation to break in excess of 600%. This behavior was demonstrated less frequently by samples containing 5% PLA, where the onset of stress oscillation was at 450% strain. Stress oscillation is known to occur in crystallizable polymers prone to extensive cold drawing, which was demonstrated by the 2% PLA samples.[24,25] That it occurred in all specimens of the 2% PLA sample and also in some of the 5% and 10% PLA loadings suggests that the PLA contributed to the manifestation of this behavior through its effect on the crystallizability of the PET. This is consistent with the observation that crystallization onset occurred at a higher temperature and therefore more readily in the samples

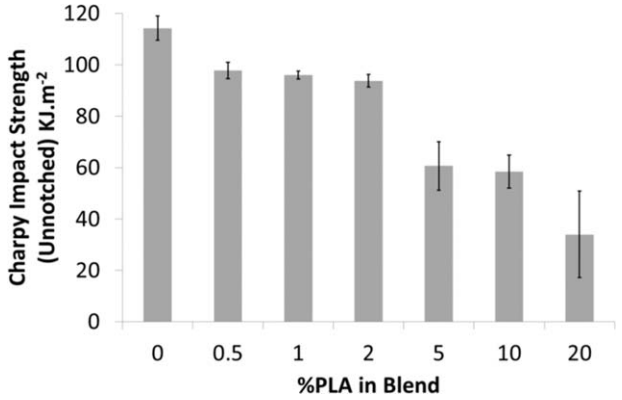

Figure 12. Charpy impact strength (unnotched) of injection molded PET/PLA blends.

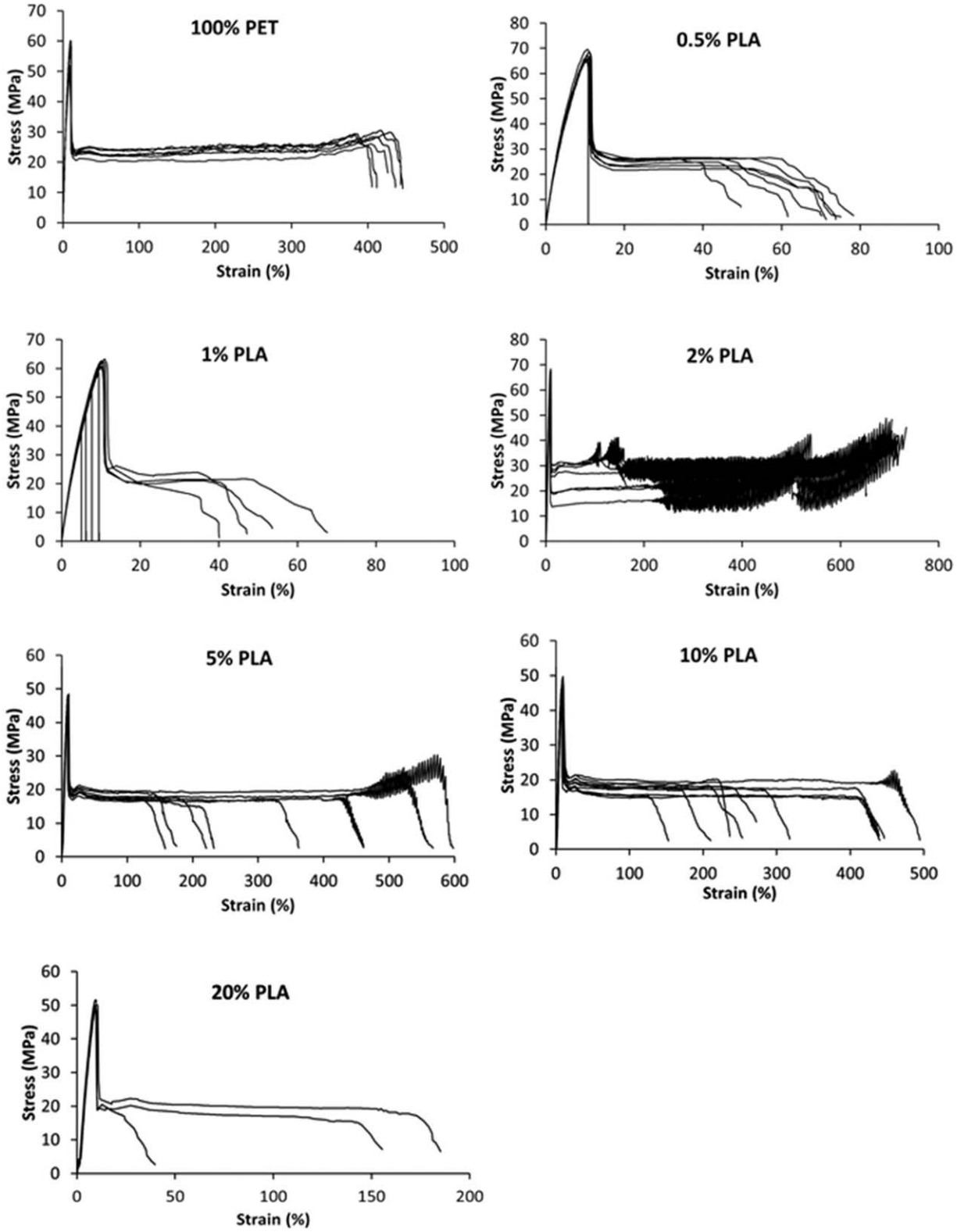

Figure 13. Stress–strain curves of injection molded blends of PET and PLA. Testing speed = 50 mm min^{-1}.

containing PLA, as strain-induced crystallization is a necessary prelude to the onset of stress oscillation.[25,26] Arnout suggested that RAF promotes strain-induced crystallization by acting as a nucleant and this is consistent with the results obtained in this study.[18] At 20% PLA however, the disruptive effect of the PLA microparticles, which were also much larger in this material, was the overriding factor resulting in failure of the material, so that no stress oscillation was apparent.

CONCLUSIONS

The effect of inclusion of PLA into PET during injection molding has been studied by thermal analysis, X-ray diffraction, scanning electron microscopy, and mechanical testing. Injection molded samples were uniformly amorphous as shown by XRD analysis and the exhibition of cold crystallization on first heating during DSC analysis. PLA enhanced the development of crystallinity during recrystallization from the melt, but not during cold crystallization, which can be explained by PLA acting as a nucleant. The impact strength and tensile properties of yield stress and ultimate tensile stress were drastically reduced by PLA when present at greater than 2% concentration and this was ascribed to the increasing population of microscopic beads of PLA, which also increased in size with increasing PLA content. The nucleation effect of PLA also induced stress oscillation behavior in samples containing 2% PLA or more, although this was negated at higher PLA content by the dense population of PLA microparticles.

ACKNOWLEDGMENTS

This article is dedicated to the memory of David Baker, whose skill in injection molding made this work possible. The research was carried out as part of the "SuperCleanQ" project, funded by Grant Agreement No. 285889 under the Seventh Framework Programme Theme SME-2011-2.

REFERENCES

1. Soroudi, A.; Jakubowicz, I. *Eur. Polym. J.* **2013**, *49*, 2839.
2. Gent, M. R.; Menendez, M.; Toraño, J.; Diego, I. *Waste Manag. Res.* **2009**, *27*, 175.
3. Dvorak, R.; Evans, R.; Kosior, E. Commercial Scale Mixed Plastics Recycling: A Report on the Technical Viability of Recycling Mixed Plastic Packaging Waste from Domestic Sources on a Commercial Scale in the UK; Oxon: Banbury, England, **2009**; p 3.
4. Oromiehie, A.; Mamizadeh, A. *Polym. Int.* **2004**, *53*, 728.
5. Franz, R.; Mauer, A.; Welle, F. *Food Addit. Contam.* **2004**, *21*, 265.
6. Welle, F. *Resour. Conserv. Recycl.* **2011**, *55*, 865.
7. La Mantia, F. P.; Botta, L.; Morreale, M.; Scaffaro, R. *Polym. Degrad. Stabil.* **2012**, *97*, 21.
8. La Mantia, F. P.; Vinci, M. *Polym. Degrad. Stabil.* **1994**, *45*, 121.
9. Zou, H.; Yi, C.; Wang, L.; Liu, H.; Xu, W. *J. Therm. Anal. Calorim.* **2009**, *97*, 929.
10. Signori, F.; Coltelli, M. B.; Bronco, S. *Polym. Degrad. Stabil.* **2009**, *94*, 74.
11. Kong, Y.; Hay, J. N. *Eur. Polym. J.* **2003**, *39*, 1721.
12. Girija, B. G.; Sailaja, R. R. N.; Madras, G. *Polym. Degrad. Stabil.* **2005**, *90*, 147.
13. Minakov, A. A.; Mordvintsev, D. A.; Schick, C. *Polymer (Guildf)* **2004**, *45*, 3755.
14. Kong, Y.; Hay, J. *Polymer (Guildf)* **2003**, *44*, 623.
15. Chen, H.; Pyda, M.; Cebe, P. *Thermochim. Acta* **2009**, *492*, 61.
16. Androsch, R.; Wunderlich, B. *Polymer (Guildf)* **2005**, *46*, 12556.
17. Rastogi, R.; Vellinga, W. P.; Rastogi, S.; Schick, C.; Meijer, H. E. H. *J. Polym. Sci. Part B: Polym. Phys.* **2004**, *42*, 2092.
18. Arnoult, M.; Dargent, E.; Mano, J. F. *Polymer (Guildf)* **2007**, *48*, 1012.
19. Pawlak, A.; Pluta, M.; Morawiec, J.; Galeski, A.; Pracella, M. *Eur. Polym. J.* **2000**, *36*, 1875.
20. Auras, R.; Harte, B.; Selke, S. *J. Sci. Food. Agric.* **2006**, *86*, 648.
21. McLauchlin, A. R.; Ghita, O.; Gahkani, A. *Polym. Test.* **2014**, *38*, 46.
22. El-Taweel, S. H.; Höhne, G. W. H.; Mansour, A. A.; Stoll, B.; Seliger, H. *Polymer (Guildf)* **2004**, *45*, 983.
23. Auras, R.; Harte, B.; Selke, S. *J. Sci. Food Agric.* **2006**, *86*, 648.
24. Leclair, A.; Favis, B. D. *Polymer (Guildf)* **1996**, *37*, 4723.
25. Roseen, R. *J. Mater. Sci.* **1974**, *9*, 929.
26. Karger-Kocsis, J.; Benevolenski, O. I.; Moskala, E. J. *J. Mater. Sci.* **2001**, *36*, 3365.